Mechanical examination and analysis of W7-X divertor module sub-structures.

M.Smirnow[a], J.Boscary[a], H.Tittes[a], W.Schubert[a], A.Peacock[a]

[a]*Max Planck Institute for Plasma Physics, EURATOM Association, Boltzmannstr. 2, 85748 Garching, Germany*

Abstract

For the long pulse operation phase, the W7-X stellarator is equipped with an actively water cooled high heat flux (HHF) divertor, consisting of parallel cooled target elements mounted in individual target modules. Due to the thermal deformation of these target elements during heat loading, the pipework that connects the target elements to the water supply manifold is subject to significant forces. Finite element calculations, for target modules TMh1-TMh2, show the superimposed forces of the whole pipework structure on to the manifold resulting in a torsional torque on the manifold support structure and weld. During manufacture, welding of the manifold to its support structure produces thermal induced distortion, resulting in difficulty in maintaining the accuracy of the manifolds. The welding between manifold and support structure was thus minimised in order to reduce this distortion. Finite element calculations showed that the nominal welds were acceptable; however, mechanical stress test on the manifolds mount point was carried out to prove the weld performance under the calculated loading conditions to ensure the safety of the component. For the remaining modules under design TMh1-TMh4 a parametric finite element calculation design study on the effect of the pipe length and routing on the stiffness helped to define minimum requirements for the design. The status of the manifolds for these modules will be shown. The manifolds are also mechanically connected to the port plug-in, therefore the impact of the thermal displacements on this pipework coming from plasma radiation affecting the target elements and from power loads coming from ECRH stray field radiation have been calculated. The paper discusses the results of the calculations and presents the outcomes of the stress test.

Keywords: Wendelstein 7-X, Stellarator, Divertor, finite element calculation

1. Introduction

For long pulse operation of the Wendelstein 7-X (W7-X) stellarator it is foreseen to install an actively water cooled high heat flux (HHF) divertor, consisting of individual target modules [1]. Each module is a set of target elements made of CFC tiles bonded to a CuCrZr heat sink, which are mounted onto a support frame. The divertor is made of 10 similar and discrete units aligned along the field lines. Each unit consists of four main areas, three HHF areas; the vertical target, the horizontal target and the high iota tail together with an intermediate section designed for a lower heat flux [2]. Each HHF target module consists of eight to twelve cooled target elements. These elements are designed to withstand a maximum heat load of $10MW/m^2$. Additional ECRH stray radiation develops by reflection and scattering of the ECRH beam on in-vessel components. Whereas thermal radiation of the plasma is almost entirely absorbed by the first wall, in-vessel components usually
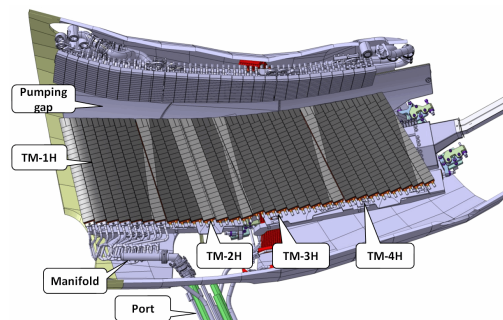

Figure 1: Birds eye view to the Divertormodule 1h-4h

have a low absorption coefficient for microwaves. The reflectivity of the first wall is in the order of about 95% (graphite) and 99% (stainless steel)[3]. The uncooled parts of the attachment frame system of the divertor absorb $300W/m^2$. The work presented here sets the focus to the divertor sub-structures that interact with the support frame.

Email address: michael.smirnow@gmail.com (M.Smirnow)

2. Design of the divertor module sub-structures

The mass of the horizontal divertor module 1-4 shown in Fig.1 is 260kg, this weight is distributed over two mechanically coupled divertor adjustment frames shown in Fig. 2. The module is comprised of target elements, mechanically attached to a module frame; the behavior of this attachment under heat load and cyclic mechanical load was already discussed in prior work [2]. The frames shown in Fig.2 connect on their lower
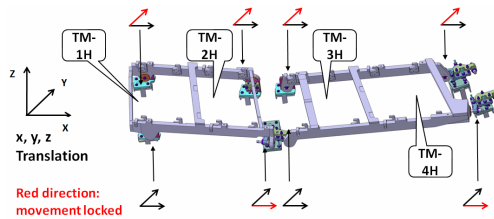

Figure 2: Degrees of freedom of the divertor frame

side to the consoles that attach them to the plasma vessel wall, on the upper side they provide a hook and clamp mechanism for easy installation of the module holder to the adjustment frame. The console connectors provide sliding supports to allow thermal expansion whereas both frame modules are coupled in one point. On top of the adjustment frame the module holders are
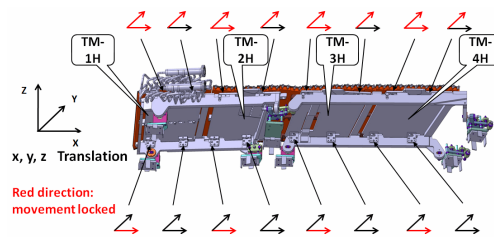

Figure 3: Degrees of freedom of the module holder

hooked into clamp able latches. The latches orientation defines the degree of freedom of the module holder as seen in Fig. 3. Those degree of freedoms avoid on the one hand thermal induced stress that might occur in a over-constrained assembly, on the other they must provide enough stiffness to avoid any leading edge phenomena of the divertor [4]. A third fixed point is realized by the cooling pipework which connect the target elements with the water supply manifolds. The manifolds are carried by two manifold holders for each manifold, visible in Fig.4.
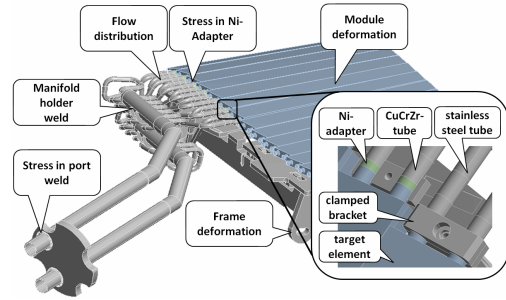

Figure 4: Highlighted points show important areas of divertor sub-structures.

3. Finite element calculations of critical areas in the divertor design

Prior calculations for the divertor [8] and [6] show that with the design load of $10MW/m^2$ and a given water velocity of $8m/s$ the target elements temperature is in the range of $800°C$ on the plasma facing CFC surface. Fig.5 shows two thermal results for the module 1h. The module is mechanically fixed on the module holder only on the water connectors side, described in [2], the other two mount stubs are sliding points. Two thermal load cases have been calculated, the centre loading above the stud and loading between the two sliding studs. In both cases the maximum
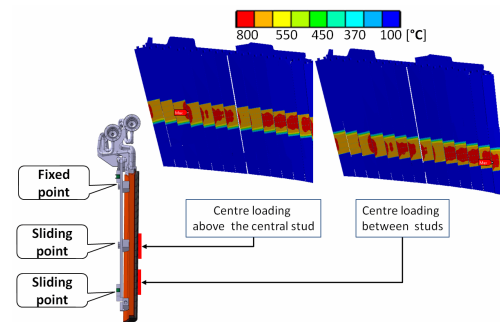

Figure 5: Results of the thermal calculation with $10MW/m^2$ load in the centre and between the mount studs.

temperature on the CFC surface did not exceed $810°C$, the uncooled target module holders heat up $60°C$. The temperature field of the two result sets was then mapped by volumetric triangulation [9] to a fine mesh for the static structural mechanical calculation.

The scope of this static structural mechanical finite element calculations was to analyse the following issues:

- Design space for pipe routing

- Stress in Ni-adapter

- Stress in manifold holder weld

Additional to the mechanical aspects, the hydraulic balance of the cooling water inlet flow was calculated and will be presented.

3.1. Two dimensional parametric study of the design space for the pipe routing

In previous designs of the divertor modules a small bellow between target element and manifold was foreseen, risk mitigation of a LOCA (loss of coolant accident) event pushed the design in a bellow free direction. This lead to the consequence of the redesign of the whole pipework in order to give the pipework the flexibility to compensate target element movements. Parametric finite element calculations have been carried out to investigate the minimal design space to retain this flexibility. Fig.6 shows the location of the two parameters - vertical length (A) and horizontal length (B) - and the corresponding response surface of the resulting stress in the cross-section of the Ni-Adapter.
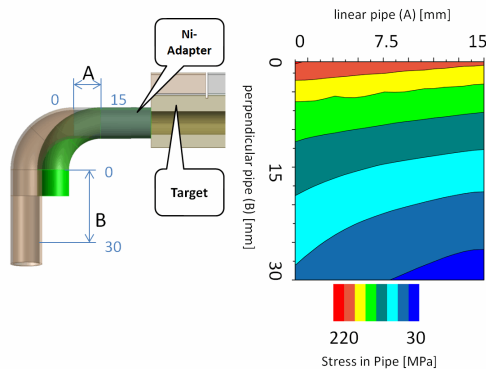

Figure 6: Target element section used for parametric pipe study.

To suppress thermal induced stress in the Ni-Adapter the perpendicular direction B is the significant parameter, Fig.6 shows that for a given bending curvature of $r/d = 1.5$ the length of B should at least exceed 30mm, what could be realized in the whole pipework for module 1-4h.

3.2. Stress in Ni-adapter

The target element is made from CuCrZr and the pipework from stainless steel, those two materials can be joined together by HIP bonding or explosion bonding [7] but for a orbital weld a Nickel adapter had to be installed in between [5], shown as sub-figure in Fig.4. Two geometry models, one with the adapter clamp, the other without have been set up and calculated with the same boundary conditions. Fig.7 shows that the effect of the adapter clamp results in a 75% reduction of stress in the Ni-adapter. The clamp divided into to halfpipe parts and is connected to the Ni-adapter with a bold that presses both parts together. In the simulation this contact was defined as a bonded contact, the assumption was validated by generating a user defined result set:

$$\frac{\sigma_s}{\sigma_n} < \mu \qquad (1)$$

Eq.1 calculates the shear-strength σ_s (contsfri) in the contact between clamp and Ni-adapter divided by the normal pressure σ_n (contstot) of this contact. The assumption is valid when this quotient is smaller then the friction factor μ of the material pair Steel-Ni.
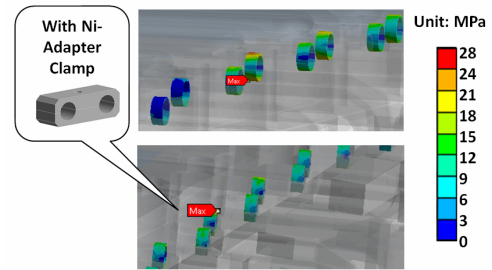

Figure 7: The adapter clamp around the Ni-Interlayer reduces the stress 75% from 30MPa to 7 MPa

It turns out that the assumption of bonded contact is valid if the friction factor of the material pair is $\mu > 0.5$ what seems realistic under vacuum conditions.

3.3. Stress in manifold holder weld

The manifold holders are welded on the manifold with a focus on a minimized heat induced distortion of the manifold to be able to respect the narrow tolerance fields of the manifold pipework. Forces from the pipework accumulate and lead to torque of the manifold. The forces have been calculated with finite element calculations and a test bed was build to proof the weld under load. Force reactions of the contacts between manifold and holder show that the accumulated force coming from the pipework is 152N. The area of the weld is $1.5 * 10mm^2$. According to the nominal stress concept, where only the flow of force is determined and correlated to the area of the weld, the stress can be calculated by:

$$\sigma_w = \frac{\Sigma F_i}{A_w} \qquad (2)$$

with σ_w as the stress in the weld, ΣF_i the accumulated forces, A_w the area of the weld. The calculated stress

results according to Eq.2 to $\sigma_w = 10 MPa$. In order of experimental test and quality assurance of the weld, a test bed was constructed around a prototype manifold, shown in Fig.8. The manifold was fixed by two base screws to a stand that was mounted to the base plate of a tensile testing machine. The hydraulic head was mounted to a push bar that pushes against the holder via two cranks. Finite element calculation of this test apparatus shows stress around $\sigma_w = 400 MPa$ in the weld for a displacement of 0.6mm. For the weld testing, the
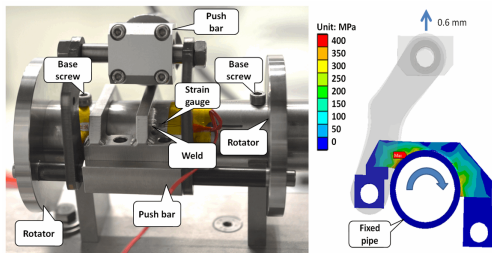

Figure 8: Testbed for the weld testing between manifold and holder (left) and the result of the v.Mises strength for the loadcase of 0.6mm displacement of the push bar (right).

tensile test bed was set up to force controlled movement and adjusted to a maximum force of 5kN at a displacement velocity of 0.065mm/s. Fig. 9 shows the linear ramp up of the force for 55s, followed by a plateau at 5kN. After 50s the force was increased for 500N, fol-
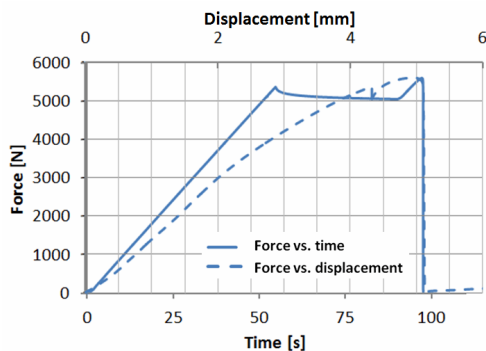

Figure 9: Force on the push bar during the weld test and its displacement response

lowed by a sudden defect of the M5 bolts that fixed the manifold to the test bed. Strain gauges placed next to the weld showed a constant maximum strain of 2.5MPa in the plateau phase. Visual examination of the weld after the test showed no indication of a crack in the weld.

4. Conclusion

Critical areas in the divertor design have been identified and analysed with finite element calculations and experiment. With a parametric study the design space was discovered that keeps the pipe stress during thermal induced strain in a safe realm. The effect of the adapter clamp around the Ni interface shows a 75% reduction of stress in this interface. The behaviour of the attachment of the manifold to the support frame under loading has been modelled and experimentally simulated. The results of this study showed that the reduced welds fulfils their function and that the attachment maintains the manifold in its position during mechanical load.

5. Acknowledgments

References

[1] *R. Stadler, A. Vorkper, J. Boscary, A. Cardella, F. Hurd, Ch. Li, et al.*,The in-vessel components of the experiment Wendelstein 7-X, Fusion Engineering and Design, **84** 305-308 (2009).

[2] *M. Smirnow, M. Kuchelmeister, J. Boscary, H. Tittes, A. Peacock*, Mechanical analysis of the joint between Wendelstein 7-X target elements and the divertor frame structure, Fusion Engineering and Design, **89** 1037-1041 (2014).

[3] *D. Hathiramani, R. Binder, R. Brakel, T. Broszat, B. Brucker, A. Cardella, M. Endler, K. Grosser, M. Hirsch, H. Laqua, S. Thiel*, Microwave stray radiation: Measures for steady state diagnostics at Wendelstein 7-X, Fusion Engineering and Design, **88** 1232-1235 (2013).

[4] *H. Renner, J. Boscary, V. Erckmann, H. Greuner, H. Grote, J. Sapper, E. Speth, F. Wesner, M. Wanner*,The capabilities of steady state operation at the stellarator W7-X with emphasis on divertor design,Nucl. Fusion, **40.6** 1083 (2000).

[5] *B. Tabernig, F. Rainer, K.H. Scheiber, B. Schedler*,Improved CuCrZr/316L transition for plasma facing components,Fus. Eng. and Design, **82** 1793-1798 (2007).

[6] *M.Y. Ye, V. Bykov, A. Peacock, F. Schauer*,Thermo-mechanical analysis of the Wendelstein 7-X divertor, Fusion Engineering and Design, **86** 1630-1633 (2011).

[7] *S.H.Goods,J.D. Puskar*,Solid state bonding of CuCrZr to 316L stainless steel for ITER applications, **86** 1634-1638 (2011).

[8] *X.B. Peng, V. Bykov, M. Köppen, M.Y. Ye, J. Fellinger, A. Peacock et al.*,Thermo-mechanical analysis of Wendelstein 7-X plasma facing components, Fusion Engineering and Design, **88** 1727-1730 (2013).

[9] *ANSYS, Inc.*, ANSYS Workbench 15 User's Guide, 2014, https://support.ansys.com/